JOURNAL OF SOLID STATE CHEMISTRY 62, 377–385 (1986)

Pyrochlore Microdomain Formation in Fluorite Oxides

M. P. VAN DIJK,* F. C. MIJLHOFF,† AND A. J. BURGGRAAF*,‡

Twente University of Technology, Department of Chemical Engineering, Laboratory for Inorganic Chemistry and Materials Science, P.O. Box 217, 7500 AE Enschede, and †State University Leiden, Gorlaeus Laboratories, P.O. Box 9502, 2300 RA Leiden, The Netherlands

Received March 11, 1985; in revised form September 30, 1985

The pyrochlore microdomain formation in the fluorite lattice was investigated by means of electron microscope techniques, especially for the system $(Tb_xGd_{1-x})_2\ Zr_2O_{7+y}$ ($0 \leqq x \leqq 1$; $0 \leqq y < 0.25$). Specimens with $x > 0.2$ or specimens with $x \leqq 0.2$ which were quenched from temperatures above the order–disorder transition temperature show diffuse scattering in the electron diffraction images, remarkably similar to diffuse scattering observed for other defect fluorite oxides. The diffuse scattering is discussed in terms of the formation of a small basic cluster in the fluorite lattice. Annealed specimens with $x \leqq 0.2$ show pyrochlore diffraction spots and microdomain formation. The domains have an average diameter ranging from a value smaller than 10 nm for $x = 0.2$ up to 100 nm for $Gd_2Zr_2O_7$. The domains grow in a disordered (fluorite) matrix and finally form antiphase boundaries. The transition from the basic cluster to a well-developed microdomain is not yet clear. The observed microdomain structure is used to explain the results of oxygen ion conductivity experiments.

Introduction

Defect fluorite oxides based on, e.g., ZrO_2,CeO_2, and HfO_2, have attracted scientific interest because of the high oxygen ion conductivity at elevated temperatures. By the introduction of lower valent cations (Ca^{2+},Mg^{2+},Y^{3+}, and various rare earth cations) in the host lattice grossly nonstoichiometric phases can be obtained in which oxygen vacancies turn out to be the mobile species. In these nonstoichiometric oxides varying states of order in the fluorite lattice are found, ranging from very small clusters and short-range order to longe-range order, which can lead to the formation of new structures. The ordering influences the oxygen ion conductivity parameters to a large extent. Rossell and Scott have given a review of experimentally observed ordering effects in these defect fluorite oxides (*1*, *2*).

A number of structural studies deal with Ca and Y stabilized zirconia and hafnia. In these materials freshly quenched specimens show high conductivity ($\sigma \approx 1\ \Omega^{-1}\ m^{-1}$ at 1000 K). but on aging, superstructure features develop. In certain cases these are accompanied by monoclinic or tetragonal precipitates which generally affect the conductivity in a destructive way (*3–9*).

In this paper we report on the formation of microdomains with the pyrochlore struc-

‡ To whom correspondence should be addressed.

0022-4596/86 $3.00

ture in fluorite-type lattices. The pyrochlore structure, with stoichiometric composition $A_2B_2O_7$, can be considered as an ordered defect fluorite structure. With B = Zr this structure is found for the phases $Ln_2Zr_{1-z}O_{2-(1/2)z}$, in which Ln is a lanthanide ranging from La to Gd. Around $z = 0.5$ the homogenity range narrows going from La to Gd. The disordered defect fluorite variant is found for the compounds with rare earth elements smaller than Gd. In compounds with Nd, Sm, or Gd an order–disorder transition is found, which for $Gd_2Zr_2O_7$ is situated at about 1550°C.

For annealed samples of $Gd_2Zr_2O_7$ and in pyrochlores with larger Ln cations, the presence of microdomains with antiphase boundaries has been demonstrated by electron microscope imaging techniques, for instance, by Michel *et al.* (*10*). However, these investigators did not study the more disordered compounds. The dimensions of the domains depend on stoichiometry, type of rare earth element, and temperature treatment. It has been proposed that for stoichiometric and nonstoichiometric pyrochlore materials of this kind completely ordered domains grow coherently within a disordered matrix. This conclusion is supported by the experimental evidence that several physical properties, like unit cell axis and oxygen ion conductivity, show a gradual change in the same concentration regions where the transition from disorder to complete order is observed (*11, 12*).

$Gd_2Zr_2O_7$ in particular is the most interesting material in this series, because the oxygen conductivity (σ) increases with the degree of order in the lattice (*11, 12*). It has been found that this can be understood in terms of the existence of preferential diffusion pathways in ordered regions together with sufficient disorder to create mobile vacancies (*13*).

Mixtures of $Gd_2Zr_2O_7$ and $Tb_2Zr_2O_{7+y}$ form a homogenous solid solution series. The material can become a mixed conducting solid, in which the ratio Tb^{4+}/Tb^{3+} depends on temperature and oxygen partial pressure and determines the amount of (p-type) electronic conductivity. (*14*). Recently the authors found that ordering effects in these materials have a profound influence on the catalytic properties for oxidation reactions (*15*).

The pyrochlore structure ($Fd3m$) has twice the unit cell length of the fluorite structure. The cations are ordered on the fcc sublattice in alternating rows in ⟨110⟩ directions (16*c* and 16*d* sites). The anion sublattice is built up from three different oxygen sites, two of which are occupied (48*f* and 8*a* sites), the third site being empty (8*b*). In this way every A cation has eightfold coordination, while each B cation has sixfold coordination. All anion sites (including the empty sites) are tetrahedrally coordinated: The 8*a* site is surrounded by four A cations, the 48*f* site by two A and two B cations, while the tetrahedron formed by four B cations is empty (8*b* site). So the vancancies are arranged around the smaller B cations at distances $\frac{1}{2}\langle 111\rangle_{\text{fluorite}}$ and form a tetrahedral network. In diffraction experiments the pyrochlore superstructure gives rise to a set of extra reflections in addition to the basic fluorite reflections, provided the local volumes of ordered material are sufficiently large.

Summarizing, the present paper is directed to the study of ordering phenomena in the system fluorite–pyrochlore paying special attention to the possibility of microdomain formation. The system $(Tb_xGd_{1-x})_2Zr_2O_{7+y}$ ($0 \le x \le 1$; $0 \le y < 0.25$) is taken as a typical representative of a series of compounds with a variable degree of order and the oxygen ion conductivity in these compounds is discussed as a function of ordering degree.

Experimental

Homogenous compounds were obtained

with a wet chemical synthesis route, using citrate complexes of the constituent metal ions (*14, 16*). After pyrolysis the material was calcined at 800°C during 4–8 hr. In most cases the powders obtained were first isostatically pressed at 400 MPa and then sintered at 1550°C, to obtain dense ceramics suitable for electrical measurements (*14*). In some cases powder batches were annealed at varying temperatures.

$Gd_2Zr_2O_7$ was either quenched from 1700°C to obtain the disordered fluorite structure (as seen with X-ray analysis) or annealed at temperatures below 1550°C to obtain well-ordered specimens. $(Tb_{0.2}Gd_{0.8})_2Zr_2O_{7+y}$ was annealed at 1250°C for 2 weeks.

X-Ray powder diffraction spectra were recorded on a Philips diffractometer PW 1330. Most samples for electron microscopic investigations were prepared by crushing the ceramic specimens. Small crystallites were dispersed in alcohol and mounted on a 400-mesh copper grid, coated with a Formvar/carbon film with holes. Other samples were obtained by argon ion beam thinning of small disks, which were mechanically polished to 50-μm thickness. The disks were mounted on a copper grid, either before or after the ion beam thinning. A Siemens Elmiskop 102 electron microscope, fitted with a double tilt cartridge and operating at 100 of 125 kV, was used for examining a sample in the diffraction and the image mode.

Results

X-Ray diffraction analysis revealed that in the series $(Tb_xGd_{1-x})_2Zr_2O_{7+y}$ only $Gd_2Zr_2O_7$, annealed at temperatures below 1550°C, has the pyrochlore structure macroscopically. The superstructure reflections, however, are less sharp and are broader than the fundamental fluorite reflections. Structure refinement analysis, based on the integrated intensities, shows that no full ordering is achieved, even after long periods of annealing.

In the Tb–Gd solid solution series for $x \leqq 0.2$ faint indications of order are present in the X-ray diffraction spectra, provided the samples have been annealed below the order–disorder transition temperature. In all other cases, i.e., at higher temperatures for $x \leqq 0.2$ and at all temperatures for $x > 0.2$, only well-defined fluorite reflections are present in the X-ray diffraction spectra.

Selected area diffraction patterns in the electron microscope for various crystal zones clearly show the diffraction spots corresponding to the reciprocal lattice of the fluorite subcell for all samples. In addition to these diffraction spots either a number of superstructure reflections or diffuse scattering phenomena are present in the areas inbetween (Figs. 1, 2). The additional spots can be indexed on the basis of the pyrochlore structure. Sometimes double diffraction is observed in addition to the pyrochlore superspots.

The most intense contours of the diffuse scattering features are circles ("smoke rings") located in a plane perpendicular to the {111} reciprocal lattice vectors centered at $\frac{1}{2}\langle 111\rangle$ positions in reciprocal space (see Fig. 4). The radius of the circles differs from one compound to another. The size of the circles in our case is relatively small compared to, for instance, Ca-doped ZrO_2 [compare Ref. (*2*)]. The diffuse intensity circles are obliquely intersected by all zones of diffraction. This results in inhomogenous intensity distributions within the intersection plane (zone), or even in a pair of spots for more or less perpendicular intersections (see, for instance, [110] and [112] zones). Besides the diffuse circles, additional, but much weaker, diffuse intensity is sometimes visible in certain zones. It is, however, not yet possible to construct a more complete geometric locus in reciprocal space corresponding to this type of observed diffuse intensity.

The diffuse intensity observed for $Tb_2Zr_2O_{7+y}$ ($y = 1$) is presented in Figs. 1a, 1b, and 2a for the [110], [112], and [012] zones, respectively. The diameter of the diffuse circle can be estimated to be $0.16a^*$ from the distance between the pair of spots (a^* is the lattice vector of the fluorite reciprocal unit cell). In the [012] zone (Fig.2a)

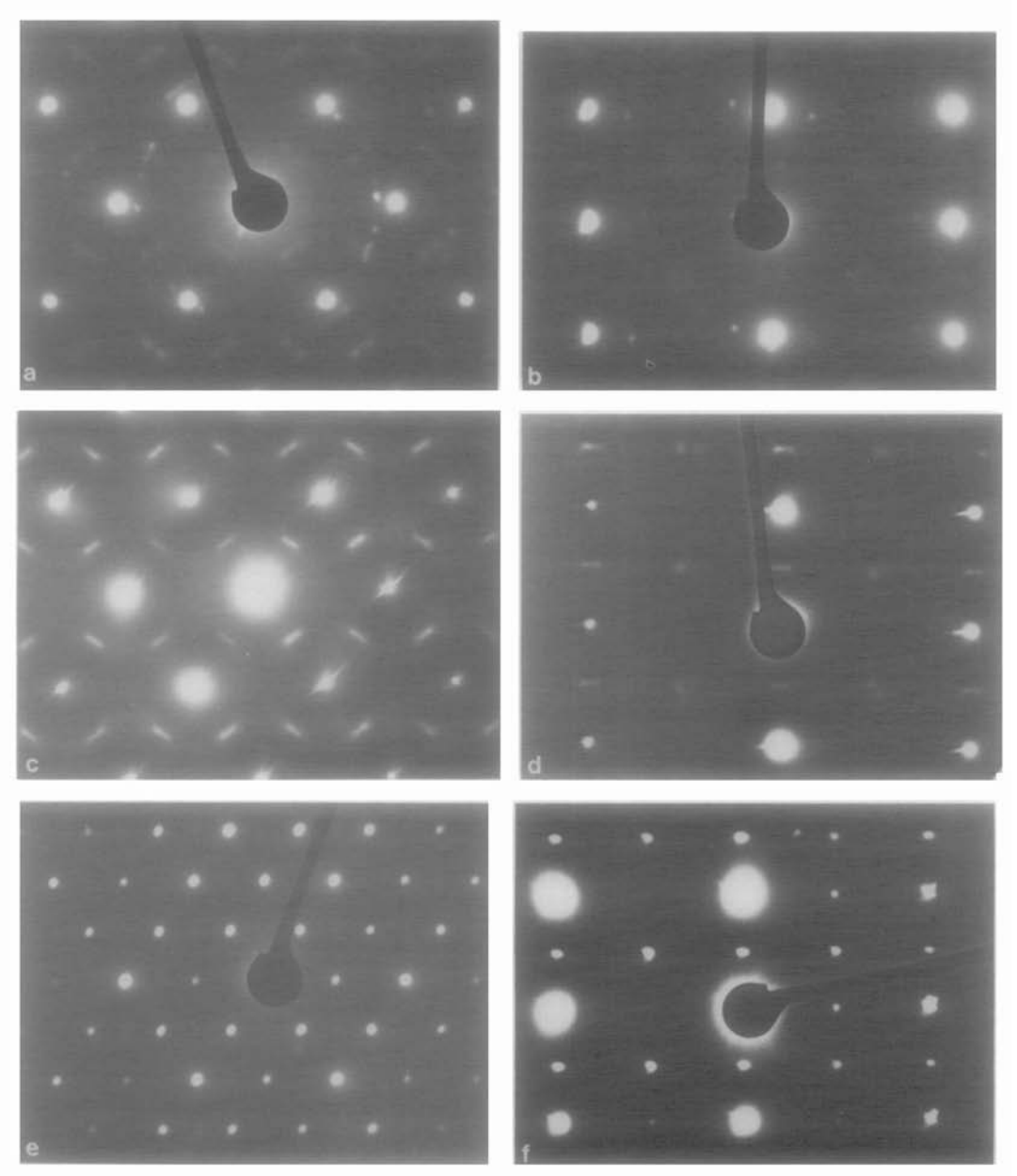

FIG. 1. Selected area diffraction patterns for the system $(Tb_xGd_{1-x})_2Zr_2O_{7+y}$. (a, b) $x = 1$; (c, d) $x = 0$, quenched sample; (e, f) $x = 0$, annealed sample (pyrochlore). a, c, and e represent the [110] zone; b, d, and f represent the [112] zone.

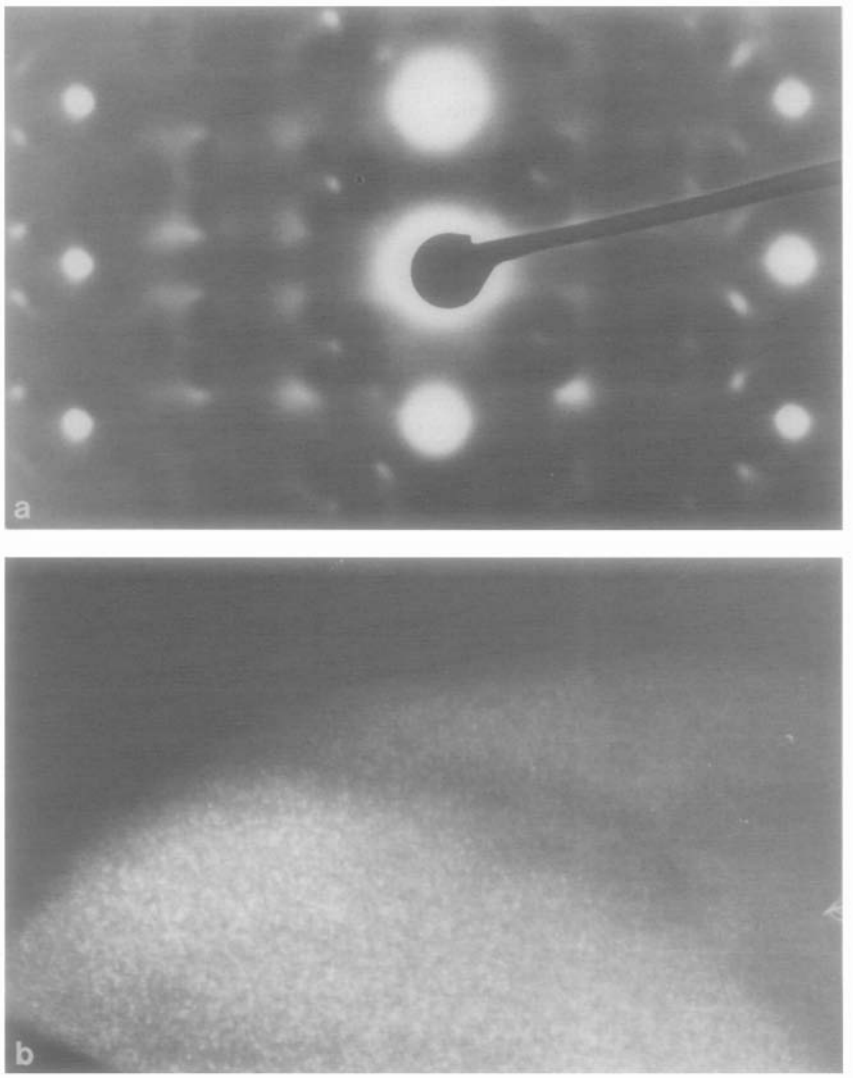

FIG. 2. Dark-field image in b, showing mottled contrast on a scale smaller than 4 nm, was constituted from the diffuse intensity of a, which represents the [012] zone for a specimen with $x = 1$.

additional diffuse scattering can be seen, connecting the diffuse circles. The dark-field image of Fig. 2b was formed by the diffuse intensity of Fig. 2a and shows a mottled contrast, suggesting the existence of regions with short-range order less than 4 nm in diameter. For compounds with $x < 1$ the same diffuse scattering features are observed, but the size of the circles is somewhat smaller. For $Gd_2Zr_2O_7$ quenched from 1700°C a circle diameter of about $0.10a^*$ was observed (Figs. 1c, d).

For annealed compounds with $0 \leqq x \leqq 0.2$ (Figs. 1e, f), the diffuse scattering has vanished and sharp superstructure spots are found at positions corresponding to the pyrochlore structure. Most of these spots (with $h + k + l = 2n + 1$) are located at the

centers of the previously discussed circles; some others (with $h + k + l = 4n$) are not. Hence going from disordered samples ($Tb_2Zr_2O_{7+y}$) to well-ordered samples ($Gd_2Zr_2O_7$, annealed), diffuse scattering circles appear to shrink to superstructure dots (compare, for instance, Figs. 1b, d, and f).

In dark-field mode, using superstructure reflections, microdomains become visible with dimensions ranging from 10 nm for $x = 0.2$ to 100 nm (Fig. 3) for $Gd_2Zr_2O_7$. In the case of $Gd_2Zr_2O_7$ this is in accordance with the results of Michel *et al.* (*10*), who also report 100 nm for $Gd_2Zr_2O_7$. For $x = 0.2$ the domains are still embedded in a disordered matrix, but for $Gd_2Zr_2O_7$ they may be regarded as domains separated by antiphase boundaries.

Discussion

In this section first the electron microscope observations are discussed in relation to the superstructure and especially the degree of pyrochlore order. Then some attention is paid to the ionic conductivity in relation to a structural model.

In the literature crystallographic models, accounting for diffuse scattering effects in solids, range from statistical descriptions of homogenous short-range order of ions or vacancies to the concept of fully ordered microdomains that exist coherently within a disordered matrix and which allow a slightly heterogenous distribution of ions. Allpress and Rossell (*3*), for instance, showed electron micrographs with mottled contrast, indicating a heterogeneous microstructure for $Ca_xM_{1-x}O_{2-x}$ (annealed specimens with M = Zr or Hf and $0.1 < x < 0.2$). They calculated that microdomains of $CaZr_4O_9$ in 12 different orientations and 2–3 nm in diameter give rise to diffuse intensity located on the circles characteristic for oxides with the defect fluorite structure. As a consequence of this model, when the domains grow larger, the diffuse intensity clusters and remains located on the (previous) circle contours. Ultimately the superspots are still located on these loci.

Indeed this was found in the case of $CaZr_4O_9$ domains and dimensions of mottled contrast correspond to the sizes of the domains used in the calculations. However, it was already noted (*2*) that there are certain difficulties with this model, as the only or-

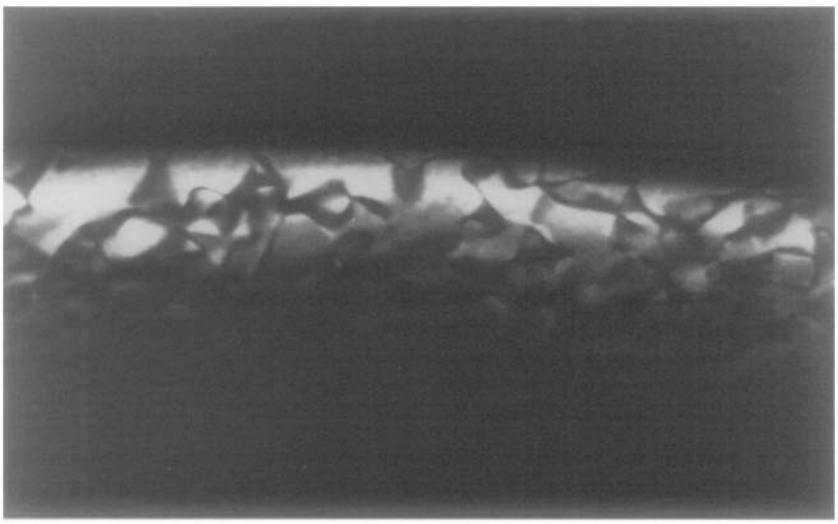

FIG. 3. Dark-field image for an annealed specimen of $Gd_2Zr_2O_7$ (pyrochlore), using superstructure reflections in the [110] zone (Fig.1e). The antiphase domains have dimensions in the range 100 nm.

dered phase known in the system ZrO_2–Y_2O_3 ($Zr_3Y_4O_{12}$) gives calculated diffuse scattering patterns different from those observed.

The observed diffuse scattering, most prominent in the [110], [012], and [112] zones and some zones with higher indices, corresponds to what has been observed for several other defect fluorite oxide systems (*1–6, 9*). Rossell already noted the remarkable similarity in symmetry of the diffuse scattering patterns observed for the different defect fluorite oxide compounds, independent of the expected limiting superstructure (*1, 2*).

Several other models have been put forward in the literature, in which relations between the microstructure and the diffuse intensity distributions in reciprocal space are discussed [e.g., Sauvage and Parthé (*18*)]. In the transition state model of De Ridder *et al.* (*19*) the diffuse scattering is attributed to predominant clusters with the macroscopic composition. If not all clusters have the bulk stoichiometry or if the number of lattice sites in the cluster is not compatible with the overall composition of the compound (e.g., in small clusters), it was deduced that the shape of the diffuse scattering will deviate from the diffuse intensity contours calculated for the ideal situation. This was illustrated by De Ridder *et al.* for examples in the alloy system Ni–Mo and this point is discussed below for the case of the fluorite pyrochlore system.

Neither the microdomain model of Allpress and Rossell (*3*), based on small parts of ideal superstructure, nor the cluster concept for simple polyhedra building up the superstructure can be applied directly to explain the diffraction features observed in the present fluorite–pyrochlore system. For both the model of Allpress and Rossell and a cluster model for simple polyhedra would require the superspots to appear on the locus in reciprocal space where the diffuse intensity was observed. However, when ordering proceeds in the fluorite–pyrochlore system the *radius* of the diffuse intensity circles changes. Moreover no simple polyhedron in the fluorite lattice can be visualized leading to the mathematical description of the diffuse circles.

In our opinion the actual cluster will be a microstructural unit or a set of closely related units being quite similar for most defect fluorite oxides. It is supposed that the microstructural unit will be based principally on the anion-vacancy sublattice and that the predominant formation of oxygen vacancy pairs at a relative distance of $\frac{1}{2}\langle 111\rangle_{\text{fluorite}}$ plays a major role in the formation of this unit. This vacancy pair is often called the "Bevan cluster" (*20*) and is generally found in structures of ordered defect fluorites (*1*). In the pyrochlore structure these vacancy pairs are linked together to form a tetrahedral network. The unknown microstructural unit is supposed to be larger than just a simple polyhedron, because of the small size of the diffuse contours. In the literature examples of the contrary have been indicated, where rather large dimensions of the diffuse contours can be coupled to small and simple polyhedra [see, e.g., Ref. (*19*)]. This unit may well be visible as the mottled contrast on a scale up to 4nm, as was found in dark-field images, using the diffuse intensity (Fig. 4).

The difference in dimension of the observed diffuse circles for samples with different amounts of Tb (different x) or different temperature treatments ($x = 0$) can now be discussed in relation to the theory of De Ridder *et al.* (*19*). It is supposed that the transition from the fluorite to the pyrochlore structure is described by a set of closely related microstructural units. One of these (perhaps the smallest) represents the general defect fluorite cluster and leads to rather large circles in the reciprocal space. On ordering, symmetry-related clusters with more and more pyrochlore character will become predominant, resulting in decreasing size of the diffuse circles and

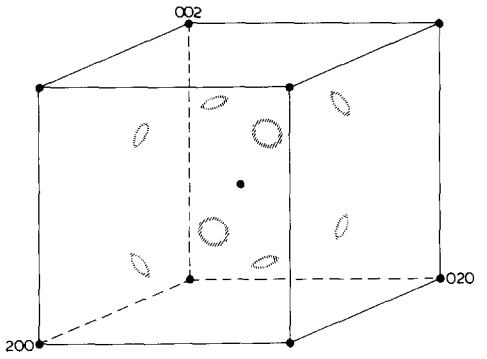

FIG. 4. Construction of the observed diffuse intensity in the fluorite reciprocal cell. Diffuse circles are located around ½(111) and have normal axis parallel to [111] direction.

ultimately in superspots at the centers of the circles.

On the other hand the variation in diameter of the circle of diffuse intensity in reciprocal space might also be induced by a variation in stoichiometry of the cluster, deviating from overall compositions as was explained by De Ridder *et al.* (*19*). In $(Tb_xGd_{1-x})_2Zr_2O_{7+y}$ this could be the result of changes in the value of y related to the observed occurrence of Tb^{4+}. This model implies that the transformation of disordered $Gd_2Zr_2O_7$ (quenched from above the order–disorder transition temperature) to well-ordered $Gd_2Zr_2O_7$ should be accompanied by a similar change in stoichiometry of the relevant cluster, because in this compound the diffuse circle decreases to a superstructure spot too. Such a change in stoichiometry is difficult to understand in $Gd_2Zr_2O_7$, because Gd does not change valency easily. Consequently variations in the diffuse intensity circles can only be correlated with intrinsic disorder.

Summarizing, it is supposed that pyrochlore order in the fluorite lattice starts from cluster formation on the anion sublattice, and proceeds by growth of these clusters, getting more and more pyrochlore stoichiometry and symmetry. Meanwhile the cations accommodate relative positions in correspondence to the pyrochlore structure. Hence, initially the pyrochlore domains will be embedded in a matrix of disordered fluorite structure, but on growing, the domains will touch. High-resolution electron microscopy might provide useful additional information about the characteristics of the transformation from clusters to microdomains and about the structure of the domain boundaries between the domains. Such a study will be performed in the near future.

The proposition, made under Results, that the domain boundaries are antiphase boundaries, can be made plausible in the following way. Michel *et al.* (*10*) showed that eight orientational variants of the pyrochlore structure exist, depending on the origin of nucleation in the fluorite matrix. Different orientational variants in touch are separated by antiphase boundaries. It was recently calculated that for the case of a [100] antiphase boundary plane, the lattice energy of such an extended defect structure is only slightly larger than the lattice energy for the perfect structure (*13*). Therefore, a structure including such antiphase boundary planes should be reasonably stable and is suggested to be present in the ordered compounds as possible pathways for rapid oxygen diffusion (*13*).

The microstructural model of pyrochlore formation presented here can now be used to explain the ionic conductivity results. Compounds with the fluorite structure found by X-ray diffraction analysis (i.e., samples quenched from high temperatures or with a large amount of Tb instead of Gd) have a relatively high value of ΔH (115–130 kJ/mol) and σ_0 (10^8–10^9 Ω^{-1} m^{-1} K) in accordance with results for the most heavily doped fluorite oxide compounds. Although electron microscopy results show that locally a certain degree of pyrochlore microdomain formation is present in these compounds and although the pyrochlore structure leads to low values of ΔH and σ_0,

this effect is hardly reflected in the conductivity parameters, because pyrochlore-like microdomains are still embedded in a disordered matrix, which dominates the conductivity results. When the domains with fully ordered pyrochlore structure have grown larger and touch each other a sharp drop in the values of ΔH and σ_0 results ($\Delta H \approx 80$–85 kJ/mol and $\sigma_0 \approx 2 \times 10^7\ \Omega^{-1}\ m^{-1}\ K$ for $Gd_2Zr_2O_7$). Now the conductivity is dominated by pathways with relatively low barrier energy in the pyrochlore structure and a small amount of free vacancies. For $Gd_2Zr_2O_7$ this results in better overall conductivity. A contribution to the conductivity mechanism from pathways along the antiphase boundary planes can be relevant too, as was shown in Ref. (*13*).

Acknowledgments

The authors acknowledge Mr. F. Schallenberg and Mr. A. de Munck (Laboratorium voor Hoogspannings Electronen Mikroskopie, Antwerp, Belgium) for their assistance in the preparation of the photographs in this paper. This investigation was supported by the Netherlands Foundation for Chemical Research (SON) with financial aid from the Netherlands Organization for the Advancement of Pure Research (ZWO).

References

1. H. J. Rossell, *in* "Advances in Ceramics" (A. H. Heuer, Ed.), Vol. 3, pp. 47–63, Amer. Ceram. Soc., Colombus, Ohio (1981).
2. H. J. Rossell and H. G. Scott, *J. Phys. C* **38,** 28 (1977).
3. J. G. Allpress and H. J. Rossell, *J. Solid State Chem.* **15,** 68 (1975).
4. B. Hudson and P. T. Moseley, *J. Solid State Chem.* **19,** 383 (1976).
5. B. Hudson and P. T. Moseley, *Inst. Phys. Conf. Ser. No. 41,* Ch. 2 (1978).
6. L. H. Schoenlein, L. W. Hobbs, and A. H. Heuer, *J. Appl. Crystallogr.* **13,** 375 (1980).
7. M. Morinaga, J. B. Cohen, and J. Faber, Jr., *Acta Crystallogr. Sect. A* **35,** 789 (1979).
8. M. Morinaga, J. B. Cohen, and J. Faber, Jr., *Acta Crystallogr. Sect. A* **36,** 520 (1980).
9. J. R. Hellmann and V. S. Stubican, *J. Amer. Ceram. Soc.* **66,** 260 (1983).
10. D. Michel, M. Perez y Jorba, and R. Collonques, *Mater. Res. Bull.* **9,** 1457 (1974).
11. M. P. van Dijk, K. J. de Vries, and A. J. Burggraaf, *Solid State Ionics* **9/10,** 913–920 (1983).
12. T. van Dijk, K. J. de Vries, and A. J. Burggraaf, *Phys. Status Solidi A* **58,** 115 (1980).
13. M. P. van Dijk, A. N. Cormack, A. J. Burggraaf, and C. R. A. Catlow, *Solid State Ionics* **17,** 159 (1985).
14. M. P. van Dijk, K. J. de Vries, and A. J. Burggraaf, *Solid State Ionics* **16,** 211 (1985).
15. J. H. H. ter Maat, M. P. van Dijk, G. Roelofs, H. Bosch, G. M. H. van de Velde, P. J. Gellings, and A. J. Burggraaf, *Mater. Res. Bull.* **19,** 1271–1249 (1984).
16. M. A. C. G. van de Graaf, T. van Dijk, M. A. de Jongh, and A. J. Burggraaf, *in* "Science of Ceramics," De Nederlandse, Keramische Vereniging (K. J. de Vries, Ed.), Enschede p. 75 (1977).
17. M. Brunel, F. de Bergevin, and M. Gondrand, *J. Phys. Chem. Solids* **33,** 1927 (1972).
18. M. Sauvage and E. Parthé, *Acta Crystallogr. Sect. A* **30,** 239 (1974).
19. R. de Ridder, G. van Tendeloo, and S. Amelinckx, *Acta Crystallogr. Sect. A* **32,** 216 (1976).
20. M. R. Thornber and D. J. M. Bevan, *J. Solid State Chem.* **1,** 536 (1970).